JOURNAL OF PETROLOGY | VOLUME 39 | NUMBER 5 | PAGES 1009–1024 | 1998

Origin of Differentiated Volcanic and Plutonic Rocks from Ascension Island, South Atlantic Ocean

A. KAR[1]*, B. WEAVER[1], J. DAVIDSON[2] AND M. COLUCCI[3]

[1]SCHOOL OF GEOLOGY AND GEOPHYSICS, UNIVERSITY OF OKLAHOMA, NORMAN, OK 73019, USA

[2]DEPARTMENT OF EARTH AND SPACE SCIENCES, UNIVERSITY OF CALIFORNIA LOS ANGELES, LOS ANGELES, CA 90095, USA

[3]DEPARTMENT OF GEOLOGY, SOUTHERN METHODIST UNIVERSITY, DALLAS, TX 75275, USA

RECEIVED MAY 31, 1997; REVISED TYPESCRIPT ACCEPTED JANUARY 28, 1998

The first phase of felsic magmatism on Ascension Island, in the form of trachyte and rhyolite domes, coulées, lava flows, and pyroclastic deposits, created the central and eastern parts of the island between about 1·0 and 0·56 my ago. The geochemical characteristics of the felsic rocks are largely consistent with an origin by fractional crystallization of high Zr/Nb mafic magmas as evidenced by identical $^{143}Nd/^{144}Nd$ and similar Pb isotopic ratios. The high Zr/Nb basalt flows constitute one of the four distinct basalt and hawaiite suites identified from Ascension based on trace element characteristics. Syenite, monzonite, and granite xenoliths associated with the felsic magmatism are interpreted as cumulate rocks from, and intrusive equivalents of, fractionating felsic magmas. Many of the felsic rocks are characterized by high $^{87}Sr/^{86}Sr$ (>0·704) compared with mafic rocks ($^{87}Sr/^{86}Sr$ <0·703), even when corrected for in situ *decay of ^{87}Rb since eruption. Such high $^{87}Sr/^{86}Sr$ coupled with high $^{143}Nd/^{144}Nd$ signatures do not correspond to known suboceanic mantle reservoirs and in the most part appear to reflect sub-solidus addition of a high $^{87}Sr/^{86}Sr$ component. This component is probably a seawater-derived fluid that might be added at the surface from wind-blown spray, or, more likely, at depth through hydrothermal circulation (fluids with high Sr contents have been recovered from fractures in a 3126-m-deep geothermal well). In either case, the extremely low Sr contents of the felsic rocks make them particularly susceptible to Sr-isotope modification. Internal (mineral) isochrons for two granite xenoliths give ages of ~0·9 and ~1·2 Ma, with initial $^{87}Sr/^{86}Sr$ >0·705. Even though the high $^{87}Sr/^{86}Sr$ signature of most of the volcanic rocks is demonstrably introduced after solidification, the high initial $^{87}Sr/^{86}Sr$ values of the granite xenoliths suggest that hydrothermally altered pre-existing volcanic basement may have been melted or assimilated during differentiation of some of the felsic magmas.*

KEY WORDS: *felsic magmatism; fractional crystallization; radiogenic isotopes; rock–magma interaction*

INTRODUCTION

Most studies of ocean island magmatism have focused on basaltic rocks and used incompatible element and isotope characteristics to define the composition(s) and melting behavior of the mantle source(s). Felsic volcanism on ocean islands is typically interpreted as the product of fractional crystallization of mafic magmas derived from hotspot-related plume sources (e.g. le Roex, 1985; Storey *et al.*, 1989), although recent detailed studies have called attention to open-system processes that may modify incompatible element and radiogenic isotopic ratios (e.g. Bohrson & Reid, 1995, 1998; Thirlwall *et al.*, 1997). Volumetrically, the occurrence of differentiated compositions in ocean island settings perhaps is under-appreciated, so understanding differentiation processes is particularly important as it will (1) determine the extent to which care must be taken in using isotope and incompatible trace element ratios indiscriminately to characterize mantle sources, and (2) define the time scales

*Corresponding author. Present address: Department of Mathematics and Physics, Fort Valley State University, Fort Valley, GA 31030, USA. Telephone: (912) 825 6844. Fax: (912) 825 6618. e-mail: kara@mail.fvsu.edu

over which mass and heat are delivered from the mantle at ocean islands.

The felsic rocks of Ascension have long been known to be characterized by unusually high $^{87}Sr/^{86}Sr$. This feature has been variously ascribed as the result of incorporation of pelagic sediment (Harris *et al.*, 1982) or altered oceanic crust (Weis *et al.*, 1987), or subsolidus alteration by seawater (Sheppard & Harris, 1985). Here we show that the felsic rocks of Ascension are largely derived by closed-system fractional crystallization, and that the Sr isotope characteristics, in most cases, reflect weathering and hydrothermal alteration of extremely low Sr rocks.

Ascension Island (7°56′S, 14°22′W) in the South Atlantic Ocean (Fig. 1), is a hotspot-related intra-plate volcanic island (Brozena, 1986). The edifice is constructed on 5–6-my-old oceanic lithosphere to the west of the Mid Atlantic Ridge, with ~1% of its volume exposed above sea level (Harris, 1983). Trachyte and rhyolite compose ~14% of the surface exposure (Nielson & Sibbett, 1996) of lava flows and pyroclastic deposits. Pyroclastic (scoria and pumice) deposits make up ~43% of the island's total areal extent (Atkins *et al.*, 1964; Harris, 1983). Also present are plutonic (granite, syenite, and monzonite) xenoliths which represent fractionation products of felsic magmas. Most of the felsic volcanic rocks and plutonic xenoliths have high initial $^{87}Sr/^{86}Sr$ compared with the mafic rocks on the island. The present study is directed to understand the petrogenesis of the felsic (>60% SiO_2) rocks and the cause of high $^{87}Sr/^{86}Sr$ in these felsic volcanic and plutonic rocks from Ascension. A more detailed consideration of the interactions involved during differentiation will be presented elsewhere.

GENERAL GEOLOGY OF ASCENSION ISLAND

Ascension is a composite volcano with >50 scoria cones scattered over the island. The exposed volcanic rocks comprise transitional to mildly alkaline basalt–hawaiite–mugearite–benmoreite–trachyte–rhyolite series [by the Le Bas *et al.* (1986) classification] lava flows, trachytic domes, scoria cones, and pyroclastic deposits (Fig. 1). Before this study, the pyroclastic deposits of mafic and felsic composition have been largely uncharacterized. In this study we geochemically and petrogenetically characterize the voluminous pumice deposits, trachyte domes, felsic lava flows, and plutonic and volcanic xenoliths.

There are two distinctive felsic eruptive centers on the island, the central felsic complex and the eastern felsic complex. The central felsic complex comprises the Middleton Ridge felsic center and Green Mountain (Fig. 1). Middleton Ridge is composed primarily of trachyte flows and pumice, and some rhyolite and rhyolitic obsidian. The highest peak on the island, Green Mountain (859 m), is made up of massive, thick pyroclastic (mostly pumice) fall deposits with the southwestern flanks mostly constituted of trachyte. The eastern felsic complex is made up of numerous trachyte flows and lava domes (Fig. 1). A voluminous trachyte lava flow originated from Devil's Cauldron and flowed northward and eastward. Devil's Cauldron is interpreted to be an explosion crater with the trachyte dome of Weather Post adjacent. Southeast of Devil's Cauldron and Weather Post is the trachytic flow dome of White Horse, to the east of which is the comenditic coulée of Little White Hill (Fig. 1). At the extreme eastern end of the island, South East Head is constituted of trachyte. In the southeastern part of Ascension small trachyte bodies occur at Round Hill, Cocoanut Bay, Ragged Hill, and Pillar Bay (Fig. 1). Trachyte from Ragged Hill and Cocoanut Bay contains unusually high modal abundance of alkali feldspar phenocrysts. In the western part of the island trachyte is found locally at Devil's Riding School, Daly's Crags, and Cross Hill (Fig. 1). Rhyolitic compositions are relatively rare, being restricted to the rhyolite flow on Middleton Ridge in the central felsic complex, Little White Hill, and a flow in the cliff section to the north of White Horse in the eastern felsic complex.

Plutonic and volcanic xenoliths

Felsic plutonic xenoliths (monzonite, syenite, and granite) and volcanic xenoliths (trachyte and rhyolite) occur mainly in pyroclastic deposits on the western flanks of Green Mountain. The granite, syenite, and monzonite xenoliths have been described in great detail by Roedder & Coombs (1967), Harris & Bell (1982), Harris *et al.* (1982), Harris (1983), Sheppard & Harris (1985), and Harris & Sheppard (1987). The granite xenoliths from Five Mile Post vary in size from a few centimeters to 25–30 cm in length; most are fine grained. Monzonite xenoliths occur on Middleton Ridge in pumice deposits and syenite xenoliths occur in the mugearite and benmoreite lava flows from Broken Tooth (Harris, 1983). Trachytic and rhyolitic xenoliths from close to Five Mile Post vary in size from a few centimeters to ~30 cm and have a laminated fabric.

Ages of evolved rocks on Ascension Island

A limited number of age dates (K–Ar) for Ascension trachyte and rhyolite exist in the literature (Harris *et al.*, 1982; Nielson & Sibbett, 1996); we have added four new Ar–Ar age dates on feldspar phenocrysts. There is a distinct clustering of ages among the exposed rocks on

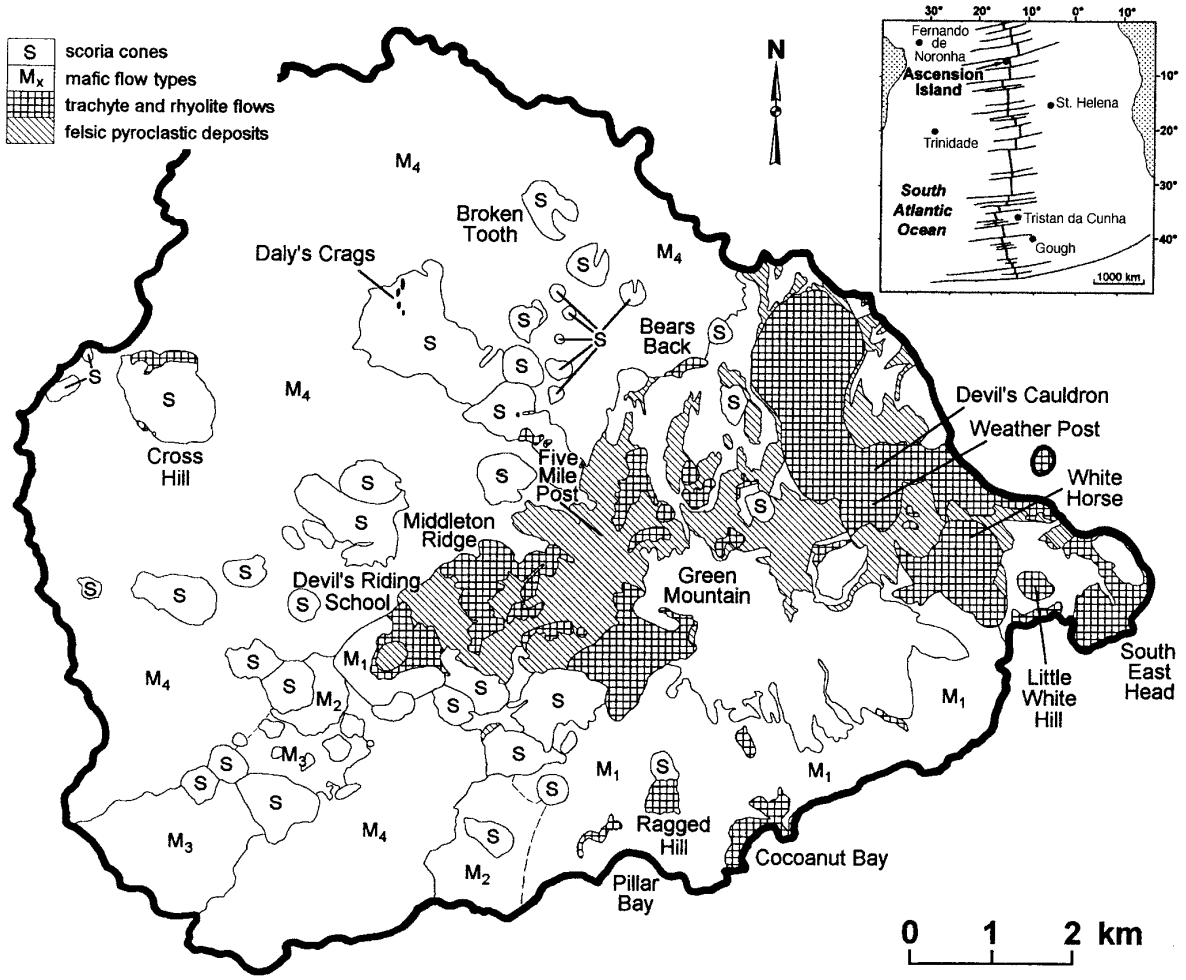

Fig. 1. Simplified geological map of Ascension Island highlighting the distribution of felsic rock types. Mafic lava flow types: M_1, high Zr/Nb basalt; M_2, Dark Slope Crater hawaiite and mugearite; M_3, low Zr/Nb hawaiite; M_4, intermediate Zr/Nb basalt to benmoreite. The inset (top right) shows the location of Ascension Island. Unshaded and unlabeled areas represent mafic ash and superficial deposits.

the island (Fig. 2), with the higher SiO_2 rocks being significantly older (range from 1·2 to 0·56 Ma) than the mafic volcanic rocks (range from 0·47 to 0·12 Ma, with a basaltic dike from Middleton Ridge dated at 0·80 Ma).

The first phase of felsic volcanism occurred in the central part of the island. A rhyolite east of Middleton Ridge is dated at 0·99 ± 0·02 Ma; this is overlain by a trachyte flow with an age of 0·82 ± 0·02 Ma and this flow is overlain by a trachyte dome closely associated with a trachyte lava flow dated at 0·65 ± 0·02 Ma (Nielson & Sibbett, 1996). From field and age relationships we suggest that the build-up of the Middleton Ridge felsic center started ~1 my ago and continued until 0·65 my ago.

Felsic magmatism next occurred:

(1) west of Middleton Ridge, where the Devil's Riding School trachyte is dated at 0·66 ± 0·02 Ma and is overlain by pumice with an age of 0·61 ± 0·02 Ma;

(2) east of Middleton Ridge, where build-up of Green Mountain occurred between 0·7 and 0·5 Ma;

(3) in the eastern felsic complex, where there is only one age date for this region, the trachyte dome of Weather Post being dated at 0·67 ± 0·02 Ma. The lack of age dates from the eastern felsic complex makes it difficult to constrain its relationship with the Middleton Ridge felsic center. The eastern felsic complex may be contemporaneous with, if not slightly younger than, the Middleton Ridge center.

These age dates suggest that the areal exposure of the central and the eastern parts of the island was built up over a period of half a million years, from ~1 Ma to

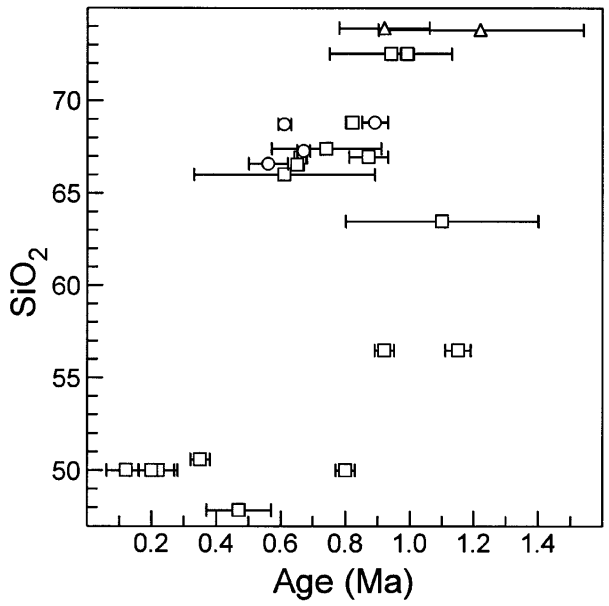

Fig. 2. Variation in SiO_2 (wt %) vs age (Ma) for mafic and felsic rocks from Ascension. Whole-rock K–Ar ages (□) are from Harris *et al.* (1982) and Nielson & Sibbett (1996) (note that for the Bears Back and Daly's Crags trachyte bodies the ages from Nielson & Sibbett are preferred to those from Harris *et al.*); Ar–Ar feldspar age dates (○) are from this study (Middleton Ridge trachyte 0·89 ± 0·04 Ma; Weather Post trachyte 0·67 ± 0·02 Ma; pumice in Devil's Riding School 0·61 ± 0·02 Ma; trachyte NNE of Mountain Red Hill 0·56 ± 0·06 Ma); Rb–Sr isochron dates for granite xenoliths (△) are from this study.

0·56 Ma. Nielson & Sibbett (1996) suggested that, as the oldest dated rocks in both the felsic complexes are rhyolite, with time the silica content of erupted felsic magma decreased as a compositionally zoned magma chamber was tapped, and that this chamber was active for >0·4 my. We note that the absence of large-volume eruptions such as caldera-related ignimbrites that are typically associated with large, long-lived magma chambers may mitigate against this possibility.

SAMPLING AND ANALYTICAL TECHNIQUES

Care was taken to obtain samples which were as fresh as possible; where practicable, the interiors of large blocks were sampled. Major and trace element data were obtained by X-ray fluorescence (XRF) and instrumental neutron activation analysis (INAA) at the University of Oklahoma, as distinguished in Table 1, with additional details given by Weaver *et al.* (1996). Sr concentrations <10 ppm compare well with more precise isotope dilution determinations. Radiogenic isotope data are given in Table 2. Sr and Pb were analyzed using a peak-hopping routine on a VG Sector mass spectrometer, whereas Nd isotope ratios were determined using a VG Sector 54-30 mass spectrometer operating in static mode. Further details have been given by Davidson *et al.* (1993). Selected data are presented in Tables 1 and 2, with the full data set available from the first author. Oxygen isotope data were obtained at SMU for whole rocks (Table 2) and two feldspar separates using the ClF_3 extraction technique described by Borthwick & Harmon (1983).

PETROGRAPHY

Trachytic rocks vary from being aphyric to very sparsely porphyritic to strongly porphyritic and mostly are massive. The most abundant phenocryst phase is alkali feldspar, with plagioclase, olivine, clinopyroxene, and titanomagnetite forming the other phenocryst or microphenocryst phases. Weaver *et al.* (1996) reported trachyte from Ragged Hill and Cocoanut Bay that has unusually high contents of alkali feldspar phenocrysts (25–35%). Feldspar phenocrysts are up to 2 mm, olivine up to 1·5 mm, and titanomagnetite and clinopyroxene are up to 0·5 mm and occur as rare clusters. Plagioclase phenocrysts are rare and tabular in shape, and range up to 2·5 mm. Some trachytic rocks contain small (0·5 mm) rounded crystals of arfvedsonite amphibole. The trachyte groundmass comprises a fine-grained felted mass of feldspar laths ranging between 0·1 and 0·2 mm, and rarely up to 1 mm and exhibiting a patchy, weak flow alignment. Rhyolitic rocks mostly are aphyric to sparsely phyric and in general massive; microphenocrysts are alkali feldspar.

DISCUSSION

Whole-rock geochemistry

Alteration of felsic rocks

Present-day Ascension has an arid climate and the felsic volcanic and plutonic rocks have no to little petrographic evidence of alteration; most chemical characteristics are therefore likely to be primary igneous ones. However, despite the apparently pristine nature of the lavas, Davidson *et al.* (1997) showed that Sr contents and isotopic compositions may have been modified, as discussed below. In contrast, pumice samples clearly are hydrated as indicated by elevated H_2O^- and loss on ignition (LOI) (Table 1) and by whole-rock $\delta^{18}O$ that ranges between +6 and +17‰ (Kar, 1997). Compared with fresh trachyte samples, most pumice samples have undergone significant loss of Na_2O (Fig. 3). The K_2O content of the pyroclastic samples is unchanged but, because of Na_2O loss, $Na_2O + K_2O$ and Na_2O/K_2O are low in pumice compared with massive trachyte flows and domes (Table 1). In addition to Na_2O loss, CaO and MgO are higher in pumice relative to trachyte (Table 1), and the

Table 1: Representative chemical analyses of felsic rocks from Ascension

	Trachyte				Rhyolite		Pumice				Granite	Syenite
	Al-111	Al-109	Al-96	Al-91	Al-95	Al-177	Al-120	Al-146	Al-174	Al-42	Al-213c	Al-187e
SiO_2	63·91	65·35	68·82	67·39	69·32	73·75	63·59	66·68	67·38	72·07	73·90	61·74
TiO_2	0·65	0·47	0·40	0·35	0·29	0·14	0·52	0·45	0·52	0·23	0·19	0·72
Al_2O_3	16·81	15·23	14·18	15·60	14·89	12·76	16·25	15·03	20·38	13·26	11·18	18·38
Fe_2O_3	4·93	5·63	4·75	4·32	4·04	2·97	5·71	5·02	4·58	4·38	4·55	5·16
MnO	0·12	0·16	0·19	0·13	0·17	0·08	0·19	0·16	0·22	0·12	0·16	0·14
MgO	0·44	0·05	0·22	0·09	0·07	0·02	0·60	0·41	0·41	0·25	<0·05	0·41
CaO	1·62	0·76	0·68	0·40	0·73	0·32	2·00	1·46	1·14	0·42	0·18	2·93
Na_2O	6·72	6·36	6·18	6·57	6·33	5·28	6·82	5·35	2·71	3·58	5·30	7·55
K_2O	4·46	5·00	4·52	5·10	4·13	4·65	4·20	5·13	2·54	5·66	4·49	2·74
P_2O_5	0·34	0·99	0·06	0·05	0·03	0·03	0·12	0·31	0·12	0·03	0·05	0·23
H_2O^-	0·27	0·42	0·29	0·47	0·23	0·12	1·16	2·77	5·98	2·35	0·07	0·15
LOI	0·95	0·58	−0·08	0·25	0·14	0·36	4·67	2·72	7·69	5·25	0·22	0·33
Ni	<2	<2	<2	2	<2	<2	2	2	2	2	<2	<2
Cr	2·0	2·1	1·7	3·2	n.d.	0·9	1·9	7·1	3·9	3·1	n.d.	n.d.
Sc	13·2	14·0	9·6	5·7	n.d.	1·4	10·3	7·4	7·4	1·7	1	10
V	19	6	5	4	3	5	5	13	9	6	19	7
Zn	71	110	167	155	148	189	149	160	311	256	150	82
Ga	28	30	34	33	30	35	28	31	25	35	38	27
Rb	63	69	87	109	82	161	75	102	73	188	157	28
Sr	184	24	10 *(10·48)*	7 *(7·08)*	15	1 *(1·53)*	114	47	74	7 *(7·26)*	5 *(4·96)*	278
Ba	1304	1153	516	219	886	24	868	220	799	21	32	1668
Th	6·40	7·61	11·1	14·3	n.d.	19·4	8·85	11·9	8·02	25·1	17	2
Pb	3	3	7	7	8	11	5	6	4	14	8	4
Zr	398	532	954	1248	1003	968	766	1074	899	1743	1752	170
Hf	7·88	10·5	20·1	22·3	n.d.	23·8	13·6	19·8	15·4	33·4	n.d.	n.d.

Table 1: continued

	Trachyte				Rhyolite		Pumice				Granite	Syenite
	Al-111	Al-109	Al-96	Al-91	Al-95	Al-177	Al-120	Al-146	Al-174	Al-42	Al-213c	Al-187e
Nb	68	98	134	184	117	212	122	130	97	261	315	42
Ta	4·59	5·83	8·06	10·4	n.d.	13·6	6·87	7·63	5·47	15·6	n.d.	n.d.
La	40·3	45·3	71·9	73·2	n.d.	91·9	62·6	72·8	100	139	269*	33*
Ce	83·2	94·5	139	165	n.d.	189	128	142	142	254	479*	61*
Nd	37·2	46·7	68·6	63·0	n.d.	81·0	59·8	67·1	100	113	289*	28*
Sm	8·10	10·2	15·6	12·9	n.d.	19·1	12·5	14·6	21·9	24·2	n.d.	n.d.
Eu	3·51	3·17	3·20	2·15	n.d.	1·21	3·61	2·10	5·59	2·31	n.d.	n.d.
Tb	1·32	1·64	2·55	2·18	n.d.	3·59	1·94	2·33	3·64	3·95	n.d.	n.d.
Yb	3·72	4·96	7·25	6·99	n.d.	11·9	5·96	7·81	11·0	11·2	n.d.	n.d.
Lu	0·51	0·69	1·00	1·02	n.d.	1·56	0·84	1·11	1·53	1·66	n.d.	n.d.
Y	45	56	85	84	91	137	69	87	151	148	242	27
$Na_2O + K_2O$	11·18	11·36	10·70	11·67	10·46	9·93	11·02	10·48	5·25	9·24	9·79	10·29
Na_2O/K_2O	1·51	1·27	1·37	1·29	1·53	1·14	1·62	1·04	1·07	0·63	1·18	2·76
Zr/Nb	5·9	5·4	7·1	6·8	8·6	4·6	6·3	8·3	9·3	6·7	5·6	4·0
La/Nb	0·59	0·46	0·54	0·40	—	0·43	0·51	0·56	1·03	0·53	0·85	0·79
Rb/Nb	0·93	0·70	0·65	0·59	0·70	0·76	0·61	0·78	0·75	0·72	0·50	0·67
K/Nb	544	424	280	230	293	182	285	328	217	180	118	542
Th/Nb	0·094	0·078	0·083	0·078	—	0·092	0·073	0·092	0·083	0·096	—	—
Zr/Y	8·8	9·5	11·2	14·9	11·0	7·1	11·1	12·3	6·0	11·8	7·2	6·3
Ce_N/Yb_N	5·7	4·8	4·9	6·0	—	4·0	5·5	4·6	3·3	5·8	—	—

Al-111, Cocoanut Bay; Al-109, Ragged Hill; Al-96, Middleton Ridge flow; Al-91, Daly's Crags; Al-95, Middleton Ridge flow; Al-177, Little White Hill flow dome; Al-120, Hummock Point; Al-146, NASA Road; Al-174, Green Mountain Road; Al-42, Devil's Riding School; Al-213c, xenolith from Five Mile Post; Al-187e, xenolith from Broken Tooth flow.

Major element oxides are recalculated to sum to 100% on an anhydrous basis. H_2O^- is weight loss after drying for 12 h at 110°C. LOI is weight loss after ignition at 950°C for 1 h (oxidation of Fe^{2+} to Fe^{3+} in near-anhydrous samples results in weight gain, expressed as negative LOI). Trace elements are in parts per million; Ni, V, Zn, Ga, Rb, Sr, Ba, Pb, Zr, Nb, and Y determined by XRF, other trace elements determined by INAA except *La, Ce, Nd determined by XRF. n.d., not determined. Isotope dilution determinations of Sr concentration are given in parentheses for those samples for which XRF Sr concentrations are <10 ppm.

Table 2: Sr, Nd, Pb, and O isotopic data for felsic rocks from Ascension

		SiO_2	$^{87}Sr/^{86}Sr$	Rb (ppm)	Sr (ppm)	$^{87}Rb/^{86}Sr$	$^{87}Sr/^{86}Sr_i$	$^{143}Nd/^{144}Nd$	ε_{Nd}	$^{206}Pb/^{204}Pb$	$^{207}Pb/^{204}Pb$	$^{208}Pb/^{204}Pb$	$\delta^{18}O$ WR
Trachyte and rhyolite													
AI-111		63·91	0·705038 ± 9	63	184	0·9904	0·705024	0·513046 ± 13	+7·96	19·665	15·668	39·332	+6·41
AI-79		66·00	0·703605 ± 10	79	29	7·879	0·703493	0·513024 ± 10	+7·53	19·669	15·615	39·232	+7·73
AI-41		66·93	0·703651 ± 9	88	15	16·97	0·703410	0·513008 ± 8	+7·22	19·587	15·606	39·031	+5·47
AI-175		66·84	0·703117 ± 8	94	24	11·33	0·702956	0·513026 ± 9	+7·57	19·669	15·624	39·194	+5·76
AI-91		67·39	0·707188 ± 11	109	7·08	44·54	0·706556	0·512992 ± 6	+6·91	19·746	15·644	39·339	+7·56
AI-109		65·35	0·705950 ± 11	69	24	8·317	0·705832	0·513007 ± 9	+7·20	19·568	15·602	39·122	+8·11
AI-67		67·28	0·703715 ± 10	117	7·37	45·91	0·703063	0·512999 ± 10	+7·04	19·693	15·636	39·264	+6·57
AI-103		66·58	0·704755 ± 11	81	4·63	50·60	0·704036	0·513055 ± 11	+8·13	19·503	15·633	39·132	+6·91
AI-96		68·82	0·704053 ± 9	87	10·48	24·01	0·703712	0·513026 ± 8	+7·57	19·626	15·630	39·236	+6·30
AI-94		72·53	0·706306 ± 14	126	2·2	165·7	0·703953	0·513027 ± 8	+7·59	—	—	—	—
AI-177		73·75	0·708917 ± 11	161	1·53	304·5	0·704593	0·513026 ± 7	+7·57	19·516	15·622	39·116	+6·52
Pumice													
AI-120		63·59	0·703255 ± 9	75	114	1·903	0·703228	0·513015 ± 8	+7·35	19·617	15·609	39·125	+9·23
AI-121		60·99	0·702898 ± 10	64	270	0·6855	0·702888	0·513025 ± 18	+7·55	19·569	15·608	39·118	+6·41
AI-44		68·72	0·706368 ± 15	115	16	20·79	0·706073	0·513027 ± 9	+7·59	19·713	15·666	39·368	+15·6
AI-43		66·95	0·703498 ± 10	83	67	3·583	0·703447	0·513000 ± 9	+7·06	—	—	—	—
AI-42		72·07	0·707603 ± 10	188	7	77·71	0·706500	0·512998 ± 8	+7·02	19·687	15·650	39·330	+16·8
Granite													
AI-213c	WR	73·90	0·706920 ± 11	152·7	4·96	89·07	0·705756	—	—	—	—	—	+5·80
	Felsic minerals		0·709250 ± 10	109·9	1·18	269·5	0·705729	—	—	—	—	—	—
	Mafic minerals		0·705850 ± 10	27·7	8·51	9·403	0·705727	—	—	—	—	—	—
AI-213d	WR	73·83	0·707210 ± 10	86·7	3·80	66·00	0·706067	0·512998 ± 8	+7·02	—	—	—	—
	Felsic minerals		0·707560 ± 16	53·2	1·75	87·87	0·706038	—	—	—	—	—	—
	Mafic minerals		0·706140 ± 10	14·4	7·41	5·610	0·706043	—	—	—	—	—	—

Sr, Nd, and Pb isotope ratios determined at UCLA. Initial $^{87}Sr/^{86}Sr$ for trachyte, rhyolite, and pumice samples was calculated using an age of 1 Ma, which probably results in over-correction for some samples (see Fig. 2). For the granite samples the isochron age (~0·9 Ma for AI-213c and ~1·2 Ma for AI-213d) was used for age correction. O isotope compositions were determined at SMU. Rb and Sr abundance determined by XRF at OU, except for granite samples for which Rb and Sr were determined by isotope dilution at UCLA, and some trachyte and rhyolite samples for which Sr (decimal point) was determined by isotope dilution at UCLA.

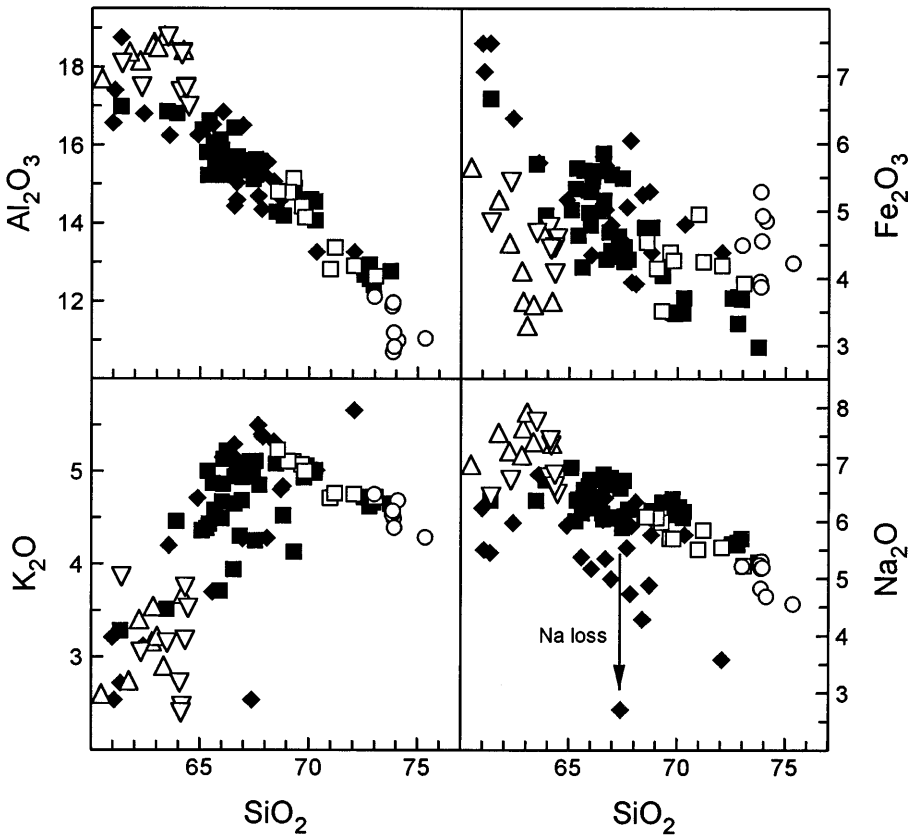

Fig. 3. Variation in SiO_2 vs Al_2O_3, Fe_2O_3, K_2O, and Na_2O (all in wt %) for felsic rocks from Ascension. Symbols plotted denote the following: △, syenite xenoliths from Broken Tooth; ▽, monzonite xenoliths from Middleton Ridge; ○, granite xenoliths from Five Mile Post; □, trachyte and rhyolite xenoliths from Green Mountain; ■, trachyte and rhyolite flows; ◆, trachyte and rhyolite pumice.

loss of Na_2O results in a significant apparent increase in SiO_2 in pumice (Table 1).

Chemical homogeneity of the felsic rocks

In a number of instances, multiple samples were collected from the same trachyte or rhyolite flow or dome (e.g. Ragged Hill, Bears Back, Middleton Ridge, Weather Post). In all cases, there are only very small variations (generally within analytical error) in the major and trace element compositions of the samples from a single flow or dome. This chemical homogeneity suggests that the lava flows and domes generally are fresh (in accord with petrographic observations) and not internally differentiated. Thus, for those flows and domes from which only a single sample was taken, the chemical composition should be representative of the unit.

Major element geochemistry

Ascension volcanic rocks are a continuous fractionation series of metaluminous alkali basalt–hawaiite–mugearite–benmoreite, to the fractionated products of peralkaline trachyte and rhyolite (Harris *et al.*, 1982; Weaver *et al.*, 1996; Kar, 1997). For felsic rock compositions (>60 wt % SiO_2; Table 1) with increase in SiO_2, Al_2O_3 constantly decreases because of crystallization of feldspar, Fe_2O_3 decreases as a consequence of olivine, clinopyroxene, and titanomagnetite crystallization, K_2O increases but becomes buffered between 65 and 70 wt % SiO_2 probably with crystallization of alkali feldspar, and Na_2O shows a slight decrease at high (>65 wt %) SiO_2 content with crystallization of alkali feldspar (Fig. 3). Most of the pumice samples have moderate to extreme depletion in Na_2O and, in general, a lower abundance of K_2O compared with the similarly differentiated lava flows and domes (Fig. 3), which is interpreted as an alteration effect (Weaver *et al.*, 1996). The Broken Tooth syenite xenoliths and the Middleton Ridge monzonite xenoliths have a limited range of chemical variation (60·5–64·5 wt % SiO_2) and generally plot on the least evolved end of fractionation trends defined by the volcanic rocks (Fig. 3). The trachyte and rhyolite xenoliths from Green Mountain have chemical compositions comparable with the exposed felsic volcanic rocks (Fig. 3). The granite xenoliths from Five Mile Post have SiO_2 in

the range 73·0–75·4 wt % and generally (Fe being a notable exception) plot on the most evolved end of major element fractionation trends defined by the felsic volcanic rocks (Fig. 3).

Harris (1983) presented a major element least-squares crystal fractionation model which showed that Ascension rhyolite compositions can be produced by simple crystal fractionation from a parental basalt magma. Harris (1983) modeled the liquid line of descent in two steps, from basalt to benmoreite (50% crystallization) and from benmoreite to rhyolite (55% crystallization). However, the basalt composition chosen by Harris (1983) is of the high Zr/Nb type [as defined by Weaver *et al.* (1996)] and is not a suitable parent to the intermediate Zr/Nb benmoreite (the flow on Letterbox) used by Harris; this is evident from the relatively poor sum of squares of residuals (0·41) and the apatite addition required by the model. Kar (1997) has shown that the different mafic magma types (high Zr/Nb, intermediate Zr/Nb, low Zr/Nb, and Dark Slope Crater) cannot be related to each other by crystal fractionation, but that the compositional variation within any one type (i.e. basalt to benmoreite in the intermediate Zr/Nb group) is consistent with a simple liquid line of descent model.

In modeling fractionation from benmoreite to rhyolite, Harris (1983) used some mineral compositions inappropriate to an intermediate to felsic system (olivine of composition Fo_{85}) and had plagioclase as the only feldspar phenocryst phase, although alkali feldspar is the predominant phenocryst in the trachytic rocks. The least-squares model of Harris (1983) has a relatively high (0·42) sum of squares of residuals. A major element least-squares (Wright & Doherty, 1970) model (Table 3) for fractionation from a trachyte with 65·7 wt % SiO_2 to a rhyolite with 69·6 wt % SiO_2 has a very low sum of squares of residuals (0·03) for a crystal extract which is dominated by alkali feldspar. However, the trace element systematics are more complicated; although the rhyolite sample (AI-95) has higher abundance of most incompatible elements than the trachyte sample (AI-126), Rb is lower in the rhyolite than in the trachyte. It must be borne in mind that these samples probably are not strictly comagmatic; felsic magmatism on Ascension spanned a period of at least 400 ky and samples AI-93 (from Middleton Ridge) and AI-126 (from near Round Hill on the southeast coast of the island) could be of very different ages and have originated from unrelated magmas which, although they fractionated similar major phenocryst assemblages and followed similar major element variation trends, had rather dissimilar trace element characteristics as a result perhaps of the crystallization of different accessory phases.

A major element least-squares model for fractionation of rhyolite AI-95 to more evolved rhyolite AI-93 (Table 3) also yields an excellent sum of squares of residuals (0·02) with a mineralogy reasonable for Ascension rhyolite (the An_{10} composition is present as a solid solution component in alkali feldspar). Both of these samples are from the felsic flow sequence on Middleton Ridge and could be comagmatic. The increase in Rb from AI-95 to AI-93 is consistent with the degree of fractionation indicated by the least-squares model if Rb is highly incompatible. Modeling of other trace elements is again complicated by the hard to quantify role of accessory phases.

The cumulate rocks that would be formed by the crystal extracts in the two least-squares models (Table 3) have major element compositions very similar to those of the syenite (Table 1) and monzonite xenoliths of Ascension.

Trace element geochemistry

Ascension felsic rocks have extremely wide variation in trace element abundance. With increasing SiO_2, Ba and Sr decrease in abundance as a result of feldspar crystallization, whereas Rb increases continuously in abundance. Both Zr and Nb generally increase in abundance with increasing SiO_2 (Fig. 4), and the plutonic xenoliths, as with major element variations, largely conform to the trends defined by the volcanic rocks. Weaver *et al.* (1996) observed that trachyte from Ragged Hill and Cocoanut Bay has high Ba and K_2O with respect to Zr and Nb compared with the rest of the Ascension suite, and interpreted this as the result of accumulation of alkali feldspar (Fig. 4); the syenite xenoliths from Broken Tooth have K/Nb higher than the volcanic rocks (Fig. 4), consistent with them being cumulate rocks from fractionation of felsic magmas. Large variations in trace element ratios, for example Zr/Nb (Fig. 4) and Zr/Y, in the felsic rocks as compared with the mafic volcanic rocks are probably due to the crystallization of accessory phases, and, in particular, the crystallization of alkali amphibole and zirconium- and rare-earth-rich accessory phases (found in the intermediate and granitic plutonic xenoliths; van Tassel, 1952; Cann, 1965), which may cause Zr bulk distribution coefficients to vary considerably during felsic magma fractionation.

The felsic rocks have extremely variable Zr/Nb, ranging from 4·6 to 9·4 (Fig. 4), although the majority of the trachyte and rhyolite samples have Zr/Nb within the range of the high Zr/Nb mafic flows (6·0–7·7). Trachyte and rhyolite of the eastern felsic complex (Weather Post, White Horse, Devil's Cauldron, Little White Hill) uniformly have Zr/Nb <6·5. The highest Zr/Nb felsic rocks are mostly in the central part of the island; the Middleton Ridge felsic rocks and the trachyte and rhyolite xenoliths from Green Mountain have Zr/Nb of 7·0–8·6 and the Devil's Riding School trachyte has the highest Zr/Nb, 9·1–9·4.

Two different fractionation trends are apparent in Fig. 4. Most trachyte samples define a trend of moderately

Table 3: Major element least-squares crystal fractionation models of the liquid line of descent for felsic compositions on Ascension

	Al-95	Ol	Plag	K-Fsp	Cpx	Mt	Ap	Al-126		Cumulate
		Fo_{30}	An_{37}	KF_3	Cpx_{14}	Mt_4		calc.	obs.	
Trachyte (Al-126) to trachyte (Al-95)										
SiO_2	69·60	32·58	59·88	67·72	52·80	0·00	0·00	65·66	65·70	62·59
TiO_2	0·29	0·00	0·13	0·04	0·72	14·05	0·00	0·45	0·56	0·59
Al_2O_3	14·95	0·00	24·88	18·70	0·26	3·05	0·00	16·69	16·70	18·15
FeO	3·65	52·24	0·43	0·26	22·00	79·75	0·00	4·21	4·19	4·70
MnO	0·17	1·99	0·01	0·01	0·63	0·47	0·00	0·12	0·12	0·08
MgO	0·07	12·90	0·08	0·00	5·21	2·68	0·00	0·29	0·36	0·47
CaO	0·73	0·29	7·37	0·06	13·13	0·00	54·90	1·36	1·37	1·88
Na_2O	6·36	0·00	6·46	7·22	5·25	0·00	0·00	6·49	6·41	6·62
K_2O	4·15	0·00	0·76	6·00	0·00	0·00	0·00	4·43	4·45	4·67
P_2O_5	0·03	0·00	0·00	0·00	0·00	0·00	41·70	0·15	0·14	0·25
Wt fraction	0·449	0·009	0·085	0·417	0·015	0·020	0·003			
								$\Sigma R^2 = 0·03$		

	Al-93	Ol	Plg	K-Fsp	Mt	Al-95		Cumulate
		Fo_5	An_{10}	KF_2	Mt_4	calc.	obs.	
Trachyte (Al-95) to rhyolite (Al-93)								
SiO_2	73·05	30·37	65·50	67·68	0·00	69·58	69·60	62·61
TiO_2	0·21	0·00	0·04	0·02	14·05	0·25	0·29	0·40
Al_2O_3	12·62	0·00	20·84	18·22	3·05	14·85	14·95	17·12
FeO	3·36	62·90	0·13	0·33	79·75	3·66	3·65	4·81
MnO	0·00	4·47	0·04	0·00	0·47	0·07	0·17	0·19
MgO	0·00	1·86	0·00	0·00	2·68	0·04	0·07	0·14
CaO	0·37	0·39	2·00	0·06	0·00	0·79	0·73	0·37
Na_2O	5·65	0·00	8·56	7·79	0·00	6·42	6·36	7·23
K_2O	4·73	0·00	2·87	5·90	0·00	4·18	4·15	4·92
P_2O_5	0·01	0·00	0·00	0·00	0·00	0·01	0·03	0·00
Wt fraction	0·661	0·013	0·270	0·048	0·007			
							$\Sigma R^2 = 0·02$	

Major element analyses recalculated to 100% with all Fe as FeO. Mineral compositions are from Harris (1983): Ol is olivine, Fo_{30} and Fo_5 from table 3, analyses 3 and 4; Plg is plagioclase, An_{37} and An_{10} from table 1, analyses 11 and 8; Cpx is clinopyroxene, Cpx_{14} from table 4, analysis 4; Mt is magnetite, Mt_4 from table 6, analysis H95(7); Ap is stoichiometric apatite, $Ca_5P_3O_{12}(OH)$. Wt fraction is the weight fraction of the phase from the least-squares model. ΣR^2 is the sum of squares of residuals (observed minus calculated oxide concentration in the parent magma) from the least-squares model. Cumulate is the composition of the bulk crystal extract in the least-squares model.

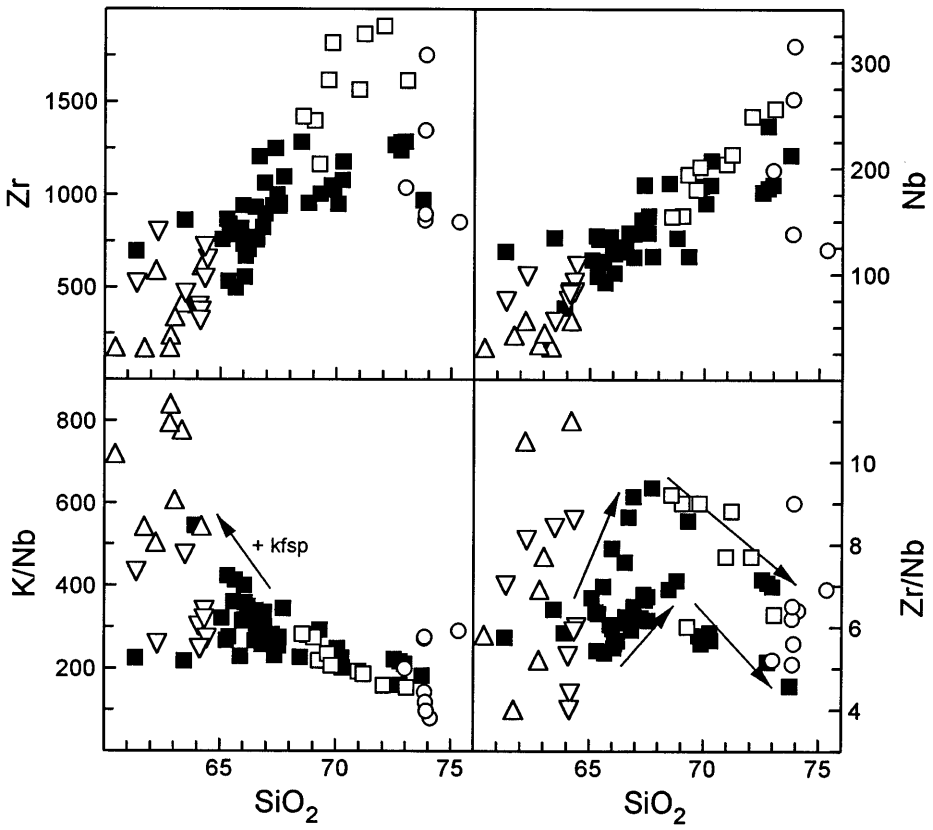

Fig. 4. Variation in Zr (ppm), Nb (ppm), K/Nb, and Zr/Nb vs SiO_2 (wt %) for felsic rocks from Ascension. Symbols as defined for Fig. 3. Two granite xenoliths which have Zr >3000 ppm and Nb >350 ppm are not plotted on the SiO_2 vs Zr and SiO_2 vs Nb diagrams. Arrows on the Zr/Nb vs SiO_2 diagram indicate the two separate fractionation trends described in the text.

increasing Zr/Nb with SiO_2 (from Zr/Nb of 5·5–6·0 at 65–66 wt % SiO_2 to Zr/Nb of ~7·0 at 69 wt % SiO_2), and then Zr/Nb decreases in the rhyolite samples from Devil's Cauldron and Weather Post (Zr/Nb 5·5–6·0 at ~70 wt % SiO_2) to the rhyolite of Little White Hill (Zr/Nb 4·6 at 73·8 wt % SiO_2). However, some trachyte samples define a separate trend of rapidly increasing Zr/Nb with SiO_2 (from Zr/Nb ~6·5 at 65 wt % SiO_2 to Zr/Nb >9·0 at 67–68 wt % SiO_2), probably the result of crystallization of an accessory phase (an Fe–Ti oxide?) with a high distribution coefficient for Nb; above ~69 wt % SiO_2, Zr/Nb falls with increasing SiO_2 because of the crystallization of zirconium silicate accessory phases.

In the plutonic rocks Zr/Nb is even more variable than in the volcanic rocks (Fig. 4), ranging from 4·0 to 13·4 in syenite, from 4·0 to 8·6 in monzonite, and from 5·1 to 9·0 in granite. Major element modeling (Table 3) indicates that the syenite and monzonite xenoliths have compositions appropriate to cumulate rocks produced by crystal fractionation of felsic magmas. Removal of a cumulate assemblage with low Zr/Nb (<5) would drive fractionating felsic liquids to higher Zr/Nb (as observed in the range from 65 to 69 wt % SiO_2; Fig. 4) whereas removal of a cumulate assemblage with high Zr/Nb (>8–10) would drive fractionating felsic liquids to lower Zr/Nb (as observed in the range above 69 wt % SiO_2). The syenite and monzonite xenoliths therefore have trace element characteristics consistent with their origin as cumulate rocks from fractionation of trachyte and rhyolite magmas. The granite xenoliths generally have major element (Fig. 3) and trace element (Fig. 4) compositions similar to the rhyolitic rocks (although some have considerably greater incompatible trace element enrichment); they are probably intrusive equivalents of the rhyolite flows and domes.

Kar *et al.* (1996) and Weaver *et al.* (1996) showed that Ascension mafic rocks have a wide variation in Zr/Nb, from 4·0 to 6·0. There are four distinct mafic (basalt to benmoreite) suites: (1) in the southwestern part of the island hawaiite flows and scoria have Zr/Nb of 4·1, (2) in the southern and the southeastern part of the island basalt flows and scoria have Zr/Nb of 5·6–6·1, (3) for the rest of the island basalt and hawaiite flows and scoria have Zr/Nb of 4·7–5·4, and (4) hawaiite and mugearite flows from Dark Slope Crater have intermediate Zr/Nb (4·9–5·4) but are distinguished by high Ni and Sr relative

to other trace elements. Data for shallow borehole samples suggest that older Ascension mafic flows have higher Zr/Nb of up to 7·7 (Kar *et al.*, 1995). The age relationship of the felsic and mafic rocks, their geographical distribution on the island, and their geochemistry, allow determination of which mafic magma type—high Zr/Nb, low Zr/Nb, intermediate Zr/Nb, or Dark Slope Crater—was parental to the felsic magmas on Ascension.

A deep (3126 m) geothermal exploration well (Ascension #1) records much of the history of the formation of the island (Nielson & Stiger, 1996). Below 1966 m, the sequence is largely mafic; felsic rocks mostly occur only above 887 m depth. Nielson & Stiger (1996) suggested that felsic volcanism is relatively recent in the growth of the volcanic edifice, although felsic rocks are the oldest exposed rocks on the island. Field observations and radiometric age dates suggest that eruption of high Zr/Nb basaltic lavas in the southeastern part of the island overlapped with the end of felsic volcanism (Weaver *et al.*, 1996), and data from the shallow boreholes (Kar *et al.*, 1995; Kar, 1997) indicate that high Zr/Nb mafic volcanism was contemporaneous with, and probably also preceded, felsic volcanism. The low Zr/Nb and Dark Slope Crater mafic flows are younger than the felsic rocks and are extremely limited in spatial distribution and volume (Weaver *et al.*, 1996); it is therefore difficult to appeal to these magma types as having produced, through fractionation, the voluminous felsic magmas erupted on Ascension. Although of substantial volume, the intermediate Zr/Nb basalt to benmoreite flows are the most recent eruptive products (Weaver *et al.*, 1996) and are highly unlikely to represent magmas parental to the earlier felsic volcanism.

The similarity in the ranges of Zr/Nb between most trachyte and rhyolite samples and the high Zr/Nb mafic rocks (5·6–7·7) suggests a genetic association. Major and trace element modeling of crystal fractionation of Ascension mafic compositions shows that there is no significant fractionation of Zr/Nb over the range from basalt to benmoreite (Kar, 1997). Therefore, from the geographical distribution, age, and behavior of incompatible element ratios of the felsic and high Zr/Nb mafic volcanic rocks, it is highly likely that the felsic magmas were derived from parental high Zr/Nb mafic magmas. Higher Zr/Nb (>8) in the felsic rocks is the result of crystal fractionation and the removal of a cumulate assemblage with low Zr/Nb, as represented by some of the syenite and monzonite xenoliths (Fig. 4). However, no intermediate (mugearite, benmoreite) products of high Zr/Nb affinity have been found, suggesting that fractionating mafic magmas either encountered a low-pressure cotectic such that copious mineral precipitation drove compositions rapidly from basalt to felsic over a small temperature range, or intermediate composition magmas encountered a density maximum in the liquid line of descent, inhibiting eruption. Major element modeling of fractionation from high Zr/Nb mafic magma to trachyte magma is too poorly constrained (the fractionation step is too large) to be of use in unequivocally establishing this petrogenetic lineage.

The rare earth element (REE) patterns of Ascension mafic and felsic volcanic rocks have slightly variable degrees of light REE (LREE) enrichment with respect to heavy REE (HREE), although the LREE are strongly enriched compared with the HREE (Kar, 1997). Continuous crystal fractionation of mafic magmas involving olivine, plagioclase, clinopyroxene, and magnetite (Harris, 1983) increases the total REE content of evolved magmas but does not produce significant inter-element fractionation (Kar, 1997). The characteristic REE pattern of the basaltic rocks is largely maintained in the more evolved rocks, although the absolute abundance has increased and substantial feldspar fractionation has produced a negative Eu anomaly (Fig. 5a). Rhyolitic compositions have a higher total abundance of REE and a larger negative Eu anomaly compared with trachyte (Fig. 5b).

When the average trachyte is normalized to average high and intermediate Zr/Nb mafic compositions (Fig. 5c and d) the MREE are strongly depleted relative to the LREE and HREE. If intermediate Zr/Nb mafic magmas were parental to trachyte magmas, it is required that $D_{LREE} > D_{HREE}$ (Fig. 5d) during fractional crystallization, which is unlikely given the fractionating phenocryst assemblage (Harris, 1983). On the other hand, production of the average trachyte from a high Zr/Nb parent magma (Fig. 5c) would require $D_{LREE} < D_{HREE}$ during crystal fractionation, which is more probable and further supports the derivation of felsic magmas from parental high Zr/Nb mafic magmas.

Isotopic data

For the most part, trachyte and rhyolite flows and pumice are isotopically similar to the mafic rocks (Table 2, Fig. 6), particularly the high Zr/Nb mafic rocks which have Zr/Nb and $^{143}Nd/^{144}Nd$ most comparable with the felsic rocks (Fig. 6). However, the most evolved trachyte and rhyolite samples have low Sr contents, high Rb/Sr, and very high Sr isotope ratios (Table 2). Undoubtedly, the high $^{87}Sr/^{86}Sr$ is in part due to *in situ* decay (Weis *et al.*, 1987), and those samples for which we have age data can be corrected for this effect (Fig. 6). Given initial $^{87}Sr/^{86}Sr$ similar to the mafic rocks (0·7028–0·7030), ages in excess of 7 Ma are required for some samples to account for the high $^{87}Sr/^{86}Sr$ felsic rocks. This is more than the maximum possible age of the rocks, as the volcanic edifice is constructed on 5–6-my-old oceanic lithosphere.

Although many of the differentiated rocks typically are characterized by high $^{87}Sr/^{86}Sr$ (>0·706), even when

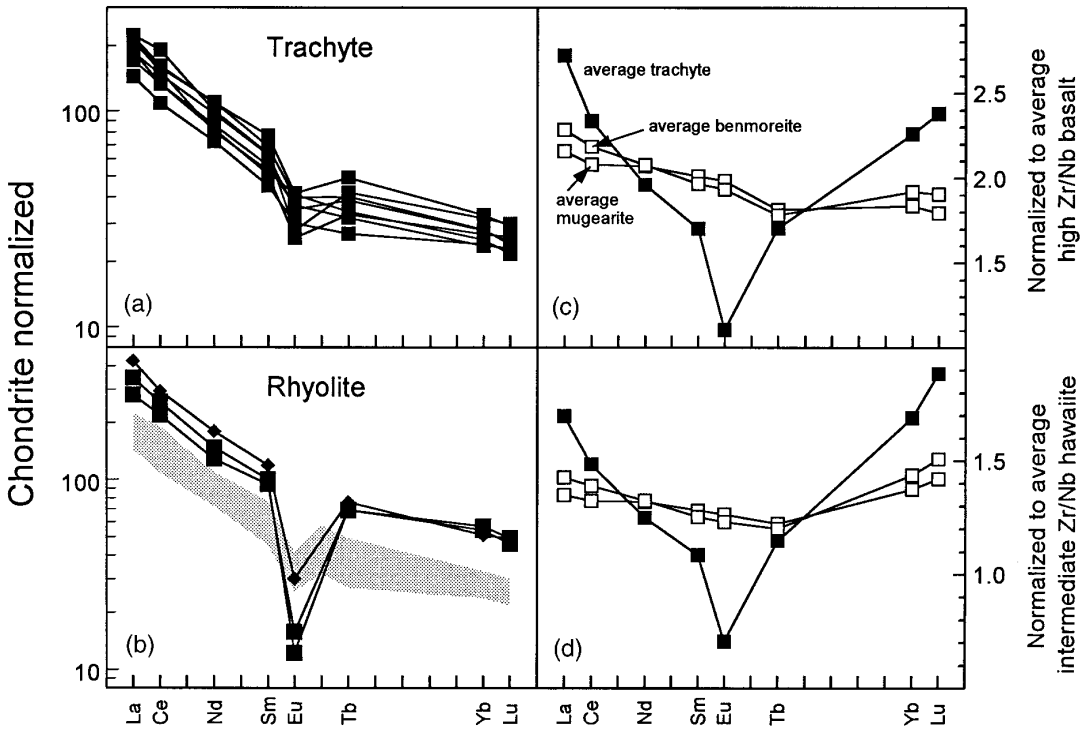

Fig. 5. Rare earth element patterns [normalized to chondrite values of Nakamura (1974)] for (a) trachyte and (b) rhyolite samples from Ascension (note, the REE patterns for the feldspar phyric trachyte of Ragged Hill and Cocoanut Bay are not shown). In (b) the shaded field shows the range of patterns for the trachyte samples. In (c) and (d) the REE patterns for average trachyte, benmoreite, and mugearite have been normalized to the REE patterns of average high Zr/Nb basalt and average intermediate Zr/Nb hawaiite, respectively.

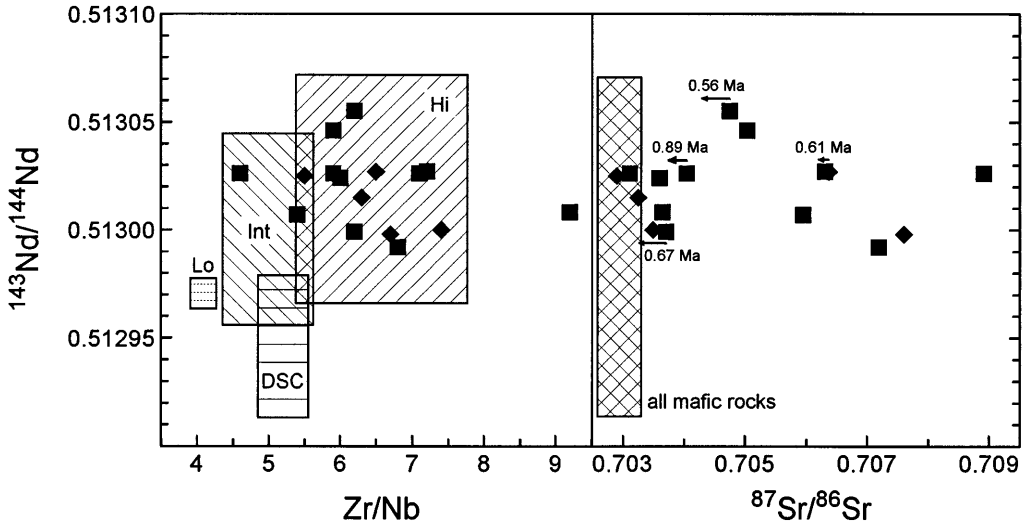

Fig. 6. Variation in Zr/Nb vs $^{143}Nd/^{144}Nd$ and in $^{87}Sr/^{86}Sr$ vs $^{143}Nd/^{144}Nd$ for Ascension felsic volcanic rocks. Symbols as in Fig. 3. Fields on the Zr/Nb vs $^{143}Nd/^{144}Nd$ plot show range of compositions of high Zr/Nb basalt (Hi), low Zr/Nb hawaiite (Lo), intermediate Zr/Nb basalt to benmoreite (Int), and Dark Slope Crater hawaiite and mugearite (DSC). For high Rb/Sr felsic samples for which ages are known, the effect of the age correction is indicated.

corrected for 1 my of aging, the narrow range of $^{143}Nd/^{144}Nd$ (and Pb isotope compositions) is similar to the range in mafic lavas that constitute most of the areal exposure of the island (Fig. 6). Such high $^{87}Sr/^{86}Sr$ and high $^{143}Nd/^{144}Nd$ signatures do not correspond to known suboceanic mantle reservoirs. Therefore, we infer that radiogenic Sr was added through crustal or hydrothermal processes. Cousens *et al.* (1993) showed that Rb and Sr can be mobilized in felsic rocks during post-eruptive processes although Pb–Nd isotopic systematics are not disturbed, and they stressed that extreme caution should be exercised when using Sr signatures as indicators of mantle-derived products. The susceptibility of the Ascension felsic rocks to secondary alteration of $^{87}Sr/^{86}Sr$ is enhanced by their low Sr contents.

This possibility of subsolidus alteration affecting Sr isotope systematics was examined by Davidson *et al.* (1997) using leaching experiments and isotopic analyses of feldspar phenocrysts. In principle, if the high $^{87}Sr/^{86}Sr$ reflects secondary alteration, this component might be leachable, and would preferentially affect groundmass rather than cleaned phenocryst separates. For most of the felsic rocks examined, a high $^{87}Sr/^{86}Sr$, relatively high Sr component was removed by acid leaching, producing residues that have Sr isotope compositions similar to the basaltic rocks when reasonable age corrections are applied. Feldspar separates, where analyzed, also have lower $^{87}Sr/^{86}Sr$, comparable with the range of basaltic rocks.

West & Leeman (1987) reported that the Holua trachyte (Hawaii) whole rock has an unusually radiogenic initial $^{87}Sr/^{86}Sr$ (0·70426) which contrasts strongly with the ratio measured on fresh feldspar phenocrysts (0·70367), and proposed prolonged interaction of the trachyte with migrating ground waters that had mixed with seawater. Similar effects have also been reported by Bohrson & Reid (1997) for peralkaline felsic rocks of Socorro Island, Mexico, where the degree of Sr isotopic disequilibrium between feldspar and whole rock increases with the age of the rocks.

We propose that the high $^{87}Sr/^{86}Sr$ in the felsic rocks of Ascension is generated by interaction of the felsic rocks with geothermal fluids derived from seawater, similar to fluids encountered in fractures of the deep (3126 m) geothermal well (Ascension #1 well) (Adams, 1996). The geothermal system below Ascension is hosted by faults and fractures (Nielson & Stiger, 1996), and two significant zones of fluid entry were encountered in Ascension #1, at 2475–2604 m depth and at 2889–2957 m depth. Fluids from both of these entries were derived from seawater and had Sr contents varying between 0·1 and 112 ppm (water sample collected during drilling) and between 9·7 and 202 ppm (water sample collected after drilling was completed). We therefore concur with previous workers in recognizing the modification of isotope characteristics in evolved ocean-island magmas, and suggest that they cannot be carelessly used to elucidate the mantle sources of ocean islands.

Nevertheless, secondary alteration cannot be the only process responsible for the high $^{87}Sr/^{86}Sr$ ratios of some of the felsic rocks, as some of the feldspar phenocrysts and residues from leaching still have $^{87}Sr/^{86}Sr$ greater than the range of the basalts. Particular insights are gained from analysis of the plutonic rocks.

Two granite xenoliths from Five Mile Post (Table 2) yield internal mineral Rb–Sr isochrons with ages of approximately (pending precise isotope dilution determination of Rb) 0·9 Ma and 1·2 Ma, respectively, and with initial $^{87}Sr/^{86}Sr$ close to 0·706; $^{143}Nd/^{144}Nd$ in one of the xenoliths is similar to the felsic extrusive rocks (Table 2). Sheppard & Harris (1985) suggested that some granite xenoliths with high $^{87}Sr/^{86}Sr$ compared with the 0·7029 initial ratio of basalt (Harris *et al.*, 1982) are either significantly older (up to 4·5 Ma) than the volcanic rocks or the granite magma was contaminated with radiogenic Sr from seawater, oceanic crust, or sediment. The isochron ages appear to preclude the former interpretation (unless significantly older granite xenoliths were simply not sampled in the current study) and implicate high magmatic $^{87}Sr/^{86}Sr$ for at least some of the felsic rocks.

The origin of the high $^{87}Sr/^{86}Sr$ magmatic signature will be discussed in more detail elsewhere. In the current presentation, we simply conclude that, like the secondary component added to most of the low Sr felsic rocks, it is ultimately seawater derived. Given that a combination of secondary alteration and aging can clearly elevate the $^{87}Sr/^{86}Sr$ of high Rb/Sr, low Sr volcanic rocks, melting of these lithologies may produce magmas with high $^{87}Sr/^{86}Sr$, from which minerals with high $^{87}Sr/^{86}Sr$ will crystallize, as appears to be the case at least for the two granite samples examined. This conclusion is consistent with hydrogen isotope systematics of Ascension granite xenoliths discussed by Sheppard & Harris (1985), which indicate that water in the original magma was seawater or meteoric derived (rather than mantle-derived magmatic).

Whole-rock oxygen isotope analyses of most of the felsic rocks have been determined and are presented in Table 2. Conceding the inadequacies of whole-rock data, we have elected not to use them in quantitative modeling. Nevertheless, it is interesting to note that the whole-rock $\delta^{18}O$ values of the trachyte lavas fall within a restricted range from +5·47 to +8·11‰, with two feldspar separates falling within 0·2‰ of the host whole rock, whereas pumice samples range from +6·41‰ to +16·8‰. As might be expected, the pumice appears clearly to be modified by low-temperature exchange with meteoric water or seawater, both of which are characterized by $\delta^{18}O$ of ~0‰. This same process may also cause the distinct depletion in Na_2O observed in the pumice samples (Fig. 3). There does not appear to be a strong

correspondence, however, between the degree of O isotope and Sr isotope disequilibrium (the trachytes show at least as much diversity in $^{87}Sr/^{86}Sr$ as the pumice samples). This may indicate that Sr isotope disequilibrium involves small amounts of fluid (which do not greatly alter O-isotope compositions), perhaps during emplacement and cooling, rather than simply surface weathering. The general lack of correlation between $^{87}Sr/^{86}Sr$ and degree of vesicularity suggests that wind-blown sea spray is a less likely means of contaminant addition, as it would be expected to have a greater effect on vesicular (high surface area) samples. One whole-rock analysis (+5·8‰) of a granite block and four laser fluorination analyses of amphibole–pyroxene mineral separates from granite blocks (+4·62, +4·51, +4·21, and +3·81‰) are similar to the low $\delta^{18}O$ ratios reported by Sheppard & Harris (1985) and are consistent with the involvement of a component derived ultimately from interaction with seawater at relatively high temperature.

CONCLUSIONS

(1) The felsic (>60 wt% SiO_2) rocks from the central and eastern parts of Ascension are the oldest exposed; a rhyolite dated at 0·99 ± 0·02 Ma (Nielson & Sibbett, 1996) from the central part of the island represents evidence of the first phase of felsic volcanism. Internal Rb–Sr isochrons for two granite xenoliths yield ages of ~0·9 and ~1·2 Ma. Felsic volcanism continued until at least 0·56 ± 0·06 Ma with build-up of the central and eastern parts of the island and was preceded and closely followed by the eruption of high Zr/Nb basalt lavas.

(2) The geochemical characteristics of the felsic rocks, together with their distribution in space and time, are largely consistent with an origin by fractionation of high Zr/Nb magmas as evidenced by similar trace element ratios and Nd and Pb isotopic ratios.

(3) Trace element and isotopic compositions indicate that syenite, monzonite, and granite xenoliths found on Ascension are cumulates from, and intrusive equivalents of fractionating felsic magmas that also produced the felsic volcanic rocks.

(4) Fluids recovered from a deep geothermal well drilled on Ascension show the presence of Sr-rich seawater-derived geothermal fluids; interaction of these fluids with felsic rocks may generate high $^{87}Sr/^{86}Sr$ under subsolidus conditions.

(5) In addition, the involvement of a high $^{87}Sr/^{86}Sr$ component during magmatic differentiation of some felsic magmas is evidenced by high initial $^{87}Sr/^{86}Sr$ from the internal isochrons of the two granite xenoliths which have high initial $^{87}Sr/^{86}Sr$ (>0·705) suggesting that hydrothermally altered pre-existing volcanic basement may have been melted or cannibalized during differentiation of these magmas.

ACKNOWLEDGEMENTS

This paper is a part of a Ph.D. dissertation by Aditya Kar. The project was funded through NSF Grant EAR-9204079. Frank Ramos and Pete Holden are thanked for their assistance with Sr isotope determinations. Ar ages at UCLA were provided with the assistance of Marty Grove and Xavier Quidueller. We have benefited from discussions with Wendy Bohrson and are grateful for the comments of Dennis Geist, Chris Harris and an anonymous reviewer, which have improved the manuscript.

REFERENCES

Adams, M. C. (1996). Chemistry of fluids from Ascension #1, a deep geothermal well on Ascension Island, South Atlantic Ocean. *Geothermics* **25,** 561–579.

Atkins, F. B., Baker, P. E. & Smith, D. G. W. (1964). Oxford expedition to Ascension Island. *Nature* **204,** 722–724.

Bohrson, W. A. & Reid, M. R. (1995). Petrogenesis of alkaline basalts from Socorro Island, Mexico: trace element evidence for contamination of ocean island basalt in the shallow ocean crust. *Journal of Geophysical Research* **100,** 24555–24576.

Bohrson, W. A. & Reid, M. R. (1997). Genesis of silicic peralkaline volcanic rocks in an ocean island setting by crustal melting and open system processes; Socorro Island, Mexico. *Journal of Petrology* **38,** 1137–1166.

Bohrson, W. A. & Reid, M. R. (1998). Genesis of evolved ocean island magmas by deep and shallow level basement recycling, Socorro Island, Mexico: constraints from Th and other isotope signatures. *Journal of Petrology* **39,** 995–1008.

Borthwick, J. & Harmon, R. S. (1982). A note regarding ClF_3 as an alternative to BrF_5 for oxygen isotope analyses. *Geochimica et Cosmochimica Acta* **46,** 1665–1668.

Brozena, J. M. (1986). Temporal and spatial variability of seafloor spreading processes in the northern South Atlantic. *Journal of Geophysical Research* **91,** 497–510.

Cann, J. R. (1965). Preliminary investigations on the acid ejected blocks of Ascension Island. *Proceedings of the Geological Society, London* **1621,** 62–63.

Cousens, B. L., Spera, F. J. & Dobson, P. F. (1993). Post-eruptive alteration of felsic ignimbrites and lavas, Gran Canaria, Canary Islands: strontium, neodymium, lead, and oxygen isotopic evidence. *Geochimica et Cosmochimica Acta* **57,** 631–640.

Davidson, J. P., Boghossian, N. D. & Wilson, B. M. (1993). The geochemistry of the igneous rock suite of St Martin, northern Lesser Antilles. *Journal of Petrology* **34,** 839–866.

Davidson, J. P., Kar, A. & Weaver, B. L. (1997). The origin of extreme isotope signatures among differentiated rocks from Ascension Island. *Geological Society of America, Abstracts with Programs* **29,** A-89.

Harris, C. (1983). The petrology of lavas and associated plutonic inclusions of Ascension Island. *Journal of Petrology* **24,** 424–470.

Harris, C. & Bell, J. D. (1982). Natural partial melting of syenite blocks from Ascension Island. *Contributions to Mineralogy and Petrology* **79,** 107–113.

Harris, C. & Sheppard, S. M. F. (1987). Magma and fluid evolution in the lavas and associated granite xenoliths of Ascension Island. In: Fitton, J. G. & Upton, B. G. J. (eds) *Alkaline Igneous Rocks. Geological Society, London, Special Publication* **30,** 269–272.

Harris, C., Bell, J. D. & Atkins, F. B. (1982). Isotopic composition of lead and strontium in lavas and coarse-grained blocks from Ascension Island, South Atlantic. *Earth and Planetary Science Letters* **60,** 79–85.

Kar, A. (1997). A comprehensive geological, geochemical, and petrogenetic study of hotspot-related oceanic basalt–rhyolite series rocks from Ascension Island, South Atlantic Ocean. Unpublished Ph.D. dissertation, University of Oklahoma, Norman, 260 pp.

Kar, A., Weaver., B., Davidson, J. & Nielson, D. (1995). Geochemical characteristics of borehole samples recovered from Ascension Island, South Atlantic Ocean. *Geological Society of America, Abstracts with Programs* **27,** 6.

Kar, A., Weaver, B., Davidson, J. & Colucci, M. (1996). Petrogenesis of mafic volcanic rocks from Ascension Island. *American Geophysical Union Fall Meeting, Abstracts with Programs* **76**(46), F698.

Le Bas, M. J., Le Maitre, R. W., Streckeisen, A. & Zanettin, B. (1986). A chemical classification of volcanic rocks based on the total alkali–silica diagrams. *Journal of Petrology* **27,** 745–750.

le Roex, A. L. (1985). Geochemistry, mineralogy and magmatic evolution of the basaltic and trachytic lavas from Gough Island, South Atlantic. *Journal of Petrology* **26,** 149–186.

Nakamura, N. (1974). Determination of REE, Ba, Fe, Mg, Na and K in carbonaceous and ordinary chondrites. *Geochimica et Cosmochimica Acta* **38,** 757–775.

Nielson, D. L. & Sibbett, B. S. (1996). Geology of Ascension Island, South Atlantic Ocean. *Geothermics* **25,** 427–448.

Nielson, D. L. & Stiger, S. G. (1996). Drilling and evaluation of Ascension #1, a geothermal exploration well on Ascension Island, South Atlantic Ocean. *Geothermics* **25,** 543–560.

Roedder, E. & Coombs, D. S. (1967). Immiscibility in granitic melts indicated by fluid inclusions in ejected granite blocks of Ascension Island. *Journal of Petrology* **8,** 417–451.

Sheppard, S. M. F. & Harris, C. (1985). Hydrogen and oxygen isotope geochemistry of Ascension Island lavas and granites: variation with crystal fractionation and interaction with seawater. *Contributions to Mineralogy and Petrology* **91,** 74–81.

Storey, M., Wolff, J. A., Norry, M. J. & Marriner, G. F. (1989). Origin of hybrid lavas from Agua de Pau volcano, Sao Miguel, Azores. In: Saunders, A. D. & Norry, M. J. (eds) *Magmatism in the Ocean Basins. Geological Society, London, Special Publication* **42,** 161–180.

Thirlwall, M. F., Jenkins, C., Vroon, P. C. & Mattey, D. P. (1997). Crustal interaction during construction of oceanic islands: Pb–Sr–Nd–O isotope stratigraphy of the shield basalts of Gran Canaria. *Chemical Geology* **135,** 233–262.

van Tassel, R. (1952). Dalyite: a new potassium zirconium silicate from Ascension Island. *Mineralogical Magazine* **29,** 850–857.

Weaver, B., Kar, A., Davidson, J. & Colucci, M. (1996). Geochemical characteristics of volcanic rocks from Ascension Island, South Atlantic Ocean. *Geothermics* **25,** 449–470.

Weis, D., Demaiffe, D., Cauet, S. & Javoy, M. (1987). Sr, Nd, O and H isotopic ratios in Ascension Island lavas and plutonic inclusions; cogenetic origin. *Earth and Planetary Science Letters* **82,** 255–268.

West, H. B. & Leeman, W. P. (1987). Isotopic evolution of lavas from Haleakala Crater, Hawaii. *Earth and Planetary Science Letters* **84,** 211–225.

Wright, T. L. & Doherty, P. C. (1970). A linear programming and least squares computer model for solving petrological mixing problems. *Geological Society of America Bulletin* **81,** 1995–2008.